Available online at www.sciencedirect.com
SCIENCE DIRECT®
Journal of Chromatography A, 1070 (2005) 89–101
JOURNAL OF CHROMATOGRAPHY A
www.elsevier.com/locate/chroma

A better global resolution function and a novel iterative stochastic search method for optimization of high-performance liquid chromatographic separation

Yandi Dharmadi [a], Ramon Gonzalez [a,b,*]

[a] *Department of Chemical Engineering, Iowa State University, 1035 Sweeney Hall, Ames, IA 50011, USA*
[b] *Department of Food Science and Human Nutrition, Iowa State University, 1035 Sweeney Hall, Ames, IA 50011, USA*

Received 10 September 2004; received in revised form 9 February 2005; accepted 18 February 2005
Available online 11 March 2005

Abstract

HPLC optimization strategy consists of four elements; experimental design, retention modeling, quality criteria function, and optimum search method. In this paper we present a simple, superior alternative to general classes of classical resolution functions (*S* function) and a novel optimum search algorithm (iterative stochastic search, ISS) for HPLC optimization. Comparison of *S* with general classes of resolution-based quality criteria functions (R_s, R_p, and R_{min}) shows superior features such as correct assessment of favorable separation conditions, preservation of peak pair contributions, elimination of arbitrary cut-off values, and a unique capability to interpret absolute significance of function values through a simple inequality. The proposed ISS algorithm is more robust than standard methods and it is easily applicable to hyperdimensional optimization. ISS also shows clear advantages in its ability to correctly identify the global optimum (instead of local optimum), with higher precision, with more efficient use of computation cycles, and with easier implementation. Successful application of *S* and ISS to HPLC optimization was demonstrated in the separation of representative functionalities (sugars, alcohols, and organic acids) present in microbial fermentations. Both the optimal and pathological (worst) conditions were successfully predicted and experimentally verified.

Keywords: HPLC optimization; Retention modelling; Resolution function; Optimum search method; Experimental design; Microbial fermentation

1. Introduction

Development of an HPLC method typically involves optimization, which is identification of operating conditions (e.g., mobile phase composition, pH, and column temperature) that result in desirable outcomes such as higher plate numbers, shorter analysis times, or in the case of simultaneous analysis of multiple compounds, better peak separation. The general optimization strategy for obtaining the best peak separation consists of four consecutive but independent elements: design of experiment, retention modeling, quality criteria function, and optimum search method. The use of experimental design allows for efficient sampling of the parameter space, while retention modeling provides a continuous representation of peak positions throughout the parameter space. Examples of experimental designs in HPLC optimization include full-factorial [1], central composite [2], uniform [3], simplex lattice [4], and "PRISMA" [5] designs. For retention modeling, the empirical, quadratic model has been successfully applied in HPLC optimization by many researchers [6–8].

Before optimization begins, a quality criteria or objective function must be defined to reflect the quality/desirability of the separation. Many quality criteria functions have been used in HPLC optimization, but the pairwise resolution function is probably the most popular:

$$R_{i,j} = \frac{t_j - t_i}{(w_i/2) + (w_j/2)} \quad (1)$$

* Corresponding author. Tel.: +1 515 294 1516; fax: +1 515 294 2386.
E-mail address: ramong@iastate.edu (R. Gonzalez).

0021-9673/$ – see front matter © 2005 Elsevier B.V. All rights reserved.
doi:10.1016/j.chroma.2005.02.075

where t_i, t_j are retention times and w_i, w_j are widths of peaks i and j in units of time. Assuming peak symmetry, $R_{i,j} = 1$ means peaks i and j are barely separated. As it is not necessary to consider non-adjacent pairs i and j in the chromatogram, the global resolution function can be defined as [9]:

$$R_p = \prod_{i=1}^{n-1} R_{i,i+1} \quad (2)$$

where n is the total number of peaks, and $i = 1$ to n is peak index in order of appearance in the chromatogram. The significance of R_p is that it reaches a maximum when all of the peaks are most evenly spaced. In fact, if the t_i's are independent variables and all w_i's are equal, R_p will reach a maximum when all adjacent peaks are exactly equidistant.

Global quality criteria such as Eq. (2) serve to represent the overall quality of peak separation with a single numerical value, thereby providing a convenient measure for subsequent optimization. A potential drawback of using global quality criteria is that, unlike pairwise criteria such as Eq. (1), information about individual peaks is lost. As an example, very well-separated peak pairs ($R_{i,j} > 2$) give unduly prominent contribution to R_p, thus potentially masking penalties due to poorly separated pairs ($R_{i,j} < 0.5$). To overcome this inherent limitation, many proposed alternatives impose some sort of arbitrary upper limit on the $R_{i,j}$ values [10,11]. Another option is to consider only the pair with lowest resolution (R_{min}), focusing only on the "bottleneck" of the separation [12]. However, other pairs could be almost as badly separated, thus critical information may be lost if they are ignored. Extensive reviews of quality criteria functions used in HPLC optimization [13,14] may be of interest to the reader.

Optimum search methods used in HPLC separation can be broadly categorized into graphical and numerical methods. Graphical methods such as the window diagram [15] and overlapping resolution map [10] provide a visual representation of how the quality criteria function changes over the variable domain, from which the optimum is easily identified. In general, this can be achieved by contour (2D) or surface (3D) plots. Optimum identification by visual inspection or "eyeballing" should give rather good accuracy. However, numerical methods offer higher precision, as well as the ability to tackle higher-dimensional optimizations.

Numerical methods commonly used in HPLC optimizations are simplex [16,17] and grid search [18,19]. A simplex is a mathematical construct that consists of $d + 1$ vertices in a d-dimensional space (e.g., a triangle in 2D, a tetrahedron in 3D). Through evaluation of the quality criteria function at the vertices, the simplex is allowed to explore the parameter space by reflection, expansion, and contraction, until all of the vertices converge to an optimum. A common problem with simplex method is that the global optimum is not always achieved – the simplex can easily be trapped inside local optima [20]. The grid search method avoids this problem by a systematic and exhaustive search over the whole variable domain. Accurate results can be achieved provided that the grid size is small enough (i.e., the gridpoints are dense enough), but preferably not too small as to impose undue computational burden during optimization.

In this paper we describe a novel quality criteria function that is simpler but superior to other $R_{i,j}$-based functions, as well as a novel optimum search algorithm that is more robust than current standards and easily applicable to hyperdimensional optimization problems. Along with statistical experimental design and retention modeling, these new elements were utilized in the optimization of temperature and mobile phase concentration in HPLC separation of representative functionalities (e.g., sugars, alcohols, and organic acids) commonly present in microbial fermentation. Comparison of the new approach to established methods is given. As an aid to method development, a computer program was written for the execution of the search algorithm.

2. Experimental

2.1. HPLC instrumentation

Experiments were run on a Waters (Milford, MA, USA) HPLC system consisting of an in-line degasser AF, gradient pump 1525 with column heater, autosampler 717 plus, refractive index detector 2410, and a personal computer with Empower software for data acquisition. An HPX-87H column with 9-μm Aminex resin (sulfonated divinylbenzene–styrene copolymer) was used with a cation H pre-column cartridge (Bio-Rad, Hercules, CA, USA) for execution of ion-exclusion chromatography. Deionized water for the mobile phase and needle wash was purified using a Nanopure II system (Barnstead, Dubuque, IA, USA) to a conductivity of 18 MΩ cm and filtered through a 0.2-μm membrane (Millipore, Billerica, MA, USA). Isocratic elution for all runs was executed at flow rate = 0.45 mL/min using dilute sulfuric acid solutions as mobile phase.

2.2. Chemicals

All chemicals were obtained from Fisher Scientific (Fair Lawn, NJ, USA) unless otherwise indicated. Twelve analytes were included in the analyses, representing three functionalities commonly present in microbial fermentation broths (sugars, alcohols, and organic acids), as well as growth medium ingredients (phosphate salts).

Glucose, xylose, glycerol, ethanol, formic acid, lactic acid, succinic acid, malic acid, and fumaric acid were obtained from Absolute Standards (Hamden, CT, USA) as 1 g/L standard solutions in water. Citric acid and pyruvic acid (as sodium pyruvate) were obtained from Sigma–Aldrich (St. Louis, MO, USA). Phosphate was obtained as potassium phosphate. The column was equilibrated for at least 2 h every time changes were introduced in temperature or mobile phase composition. Injection volume was 10 μL for all runs.

2.3. Experimental design, peak width assessment, and retention modeling

To formally define the parameter space with temperature (T) and sulfuric acid concentration in the mobile phase (C) as independent variables, a central composite design was prepared using the JMP 5.0.1 software (SAS Institute, Cary, NC, USA, http://www.jmp.com/). Boundaries of the experimental domain are defined by instrument ratings and practical considerations. For temperature, the minimum value T_{min} is set to 25 °C (ambient) and the maximum T_{max} is set to the highest temperature attainable with the column heater (60 °C). The HPX-87H column has an operating pH range of 1–3, corresponding to 0.5 to >90 mM of sulfuric acid in the mobile phase. C_{min} is set to 0.5 mM accordingly, but C_{max} is set to a lower value (30 mM), as a preliminary study suggested that separation is generally better at lower sulfuric acid concentration. Scaled variables x and y are normalized temperature and concentration defined as follows:

$$x = 1.2872\left(\frac{2T - T_{max} - T_{min}}{T_{max} - T_{min}}\right) \quad (3)$$

$$y = 1.2872\left(\frac{2C - C_{max} - C_{min}}{C_{max} - C_{min}}\right) \quad (4)$$

where T is in degrees Celsius, C is in mM, and 1.2872 is the axial value corresponding to an orthogonal central composite design [21]. It is evident that Eq. (3) linearly transforms the temperature over the [T_{min}, T_{max}] range to x in the [−1.2872, 1.2872] range, and Eq. (4) does the same for the concentration.

The T and C values at the design points are reported in Table 1 with their corresponding x and y values. With the center point repeated, the total number of design points is 10. The analytes described in Section 2.2 were combined into three injection groups, so the total number of actual chromatographic runs was 30. For similar central composite designs in three- and four-dimensions, the number of design points would be 16 and 26, respectively.

Assessment of peak separation quality with $R_{i,j}$-based functions (Eq. (1)) requires not only knowledge of retention times but also peak widths, both of which are strong functions of flow rate F. Retention time is expected to vary inversely with flow rate, and systematic studies indeed have shown that flow rate does not affect selectivity [7,22]. In general, flow rate does affect peak resolution, because plate number varies with flow rate (Van Deemter theory) [23]. However, if the plate number is assumed to be constant within a certain flow rate range, by definition peak width is proportional to retention time. Our preliminary data from a three-factor design (extra dimension for F between 0.3 and 0.6 mL/min) indicate that within the ranges considered, retention times correlate perfectly with reciprocal of flow rate, and power-law fitting of peak width vs. flow rate plots results in powers very close to −1, i.e., peak width is also inversely proportional to flow rate (Fig. 1). As this supports the constant plate number assumption, flow rate is not considered in the experimental design anymore because it does not affect peak resolution/separation quality.

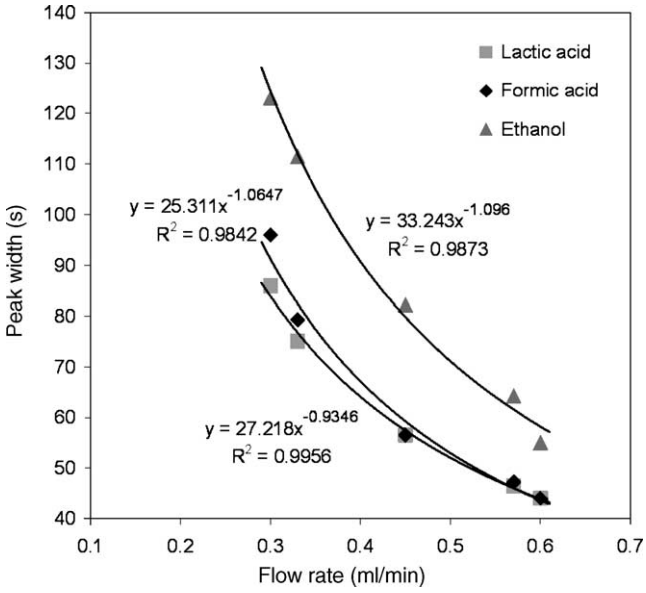

Fig. 1. Power law fitting of peak width vs. flow rate indicates hyperbolic relationship. Data for formic acid, lactic acid, and ethanol are shown.

Later in optimization, the proportionality relationship between peak width and retention time is applied with respect to a reference point (T^*, C^*), at which a preliminary run/chromatogram should be available for peak width estimates. For a given compound, the peak width at any point in the domain is then calculated as:

$$w = w(T^*, C^*)\frac{t}{t(T^*, C^*)} \quad (5)$$

where $t = t' + t_0$ is the retention time as calculated by a retention model, with t_0 (dead time) value obtained from the preliminary chromatogram. This relationship is equivalent to the constant plate number assumption. As all chromatographic runs were done at the same flow rate, t_0 is constant in this case, although generally it would vary inversely with flow rate.

To describe the retention behavior throughout the experimental domain, three retention models will be explored and evaluated at constant flow rate (0.45 mL/min). The net retention time t' can be modeled as a function of x and y with a quadratic model (model 1) [14]:

$$t'(x, y) = t - t_0 = \beta_0 + \beta_1 x + \beta_2 y + \beta_3 xy + \beta_4 x^2 + \beta_5 y^2 \quad (6)$$

where t and t_0 are the total retention time and column dead time in minutes, and β_0 to β_5 are coefficients for linear (x, y), quadratic (x^2, y^2), and interactions effects (xy) of/among temperature and concentration. Alternatively, the model is also applied to the logarithm of the capacity factor k'

Table 1
Central composite design and comparison of actual (normal font) and predicted (italics) net retention time t' in minutes at the design points

T (°C)	C (mM)	x	y	Phosphate	Malic acid	Lactic acid	Formic acid	Succinic acid	Fumaric acid	Citric acid	Pyruvic acid	Glucose	Xylose	Ethanol	Glycerol
25.0	15.25	−1.2872	0	2.630	4.583	8.233	10.282	7.747	11.796	2.524	4.895	8.714	18.758	3.098	3.918
				2.650	*4.565*	*8.254*	*10.277*	*7.748*	*12.291*	*2.510*	*4.982*	*8.694*	*18.731*	*3.082*	*3.902*
28.9	3.79	−1	−1	1.761	4.413	8.186	10.086	7.597	11.711	2.362	3.703	8.870	19.165	3.245	4.064
				1.868	*4.369*	*8.158*	*10.052*	*7.469*	*11.236*	*2.325*	*3.635*	*8.914*	*19.226*	*3.278*	*4.096*
28.9	26.71	−1	1	3.021	4.484	8.230	10.197	7.531	11.713	2.466	5.295	8.761	19.243	3.093	3.916
				2.944	*4.521*	*8.254*	*10.223*	*7.594*	*12.008*	*2.498*	*5.326*	*8.749*	*19.228*	*3.086*	*3.909*
42.5	0.5	0	−1.2872	0.832	3.301	7.450	8.684	6.125	6.749	1.434	1.404	9.237	20.398	3.549	4.366
				0.553	*3.318*	*7.457*	*8.695*	*6.162*	*6.777*	*1.451*	*1.096*	*9.174*	*20.306*	*3.503*	*4.321*
42.5	15.25	0	0	3.046	4.306	8.226	9.964	7.033	11.003	2.374	5.192	8.953	20.095	3.303	4.126
				3.046	4.307	8.227	9.965	7.026	11.002	2.376	5.194	8.956	20.095	3.299	4.121
				3.095	*4.300*	*8.202*	*9.958*	*7.042*	*10.722*	*2.366*	*5.212*	*8.961*	*20.106*	*3.306*	*4.128*
42.5	30.0	0	1.2872	3.410	4.268	8.211	9.948	6.976	11.248	2.347	5.673	8.946	20.282	3.242	4.066
				3.352	*4.321*	*8.216*	*9.982*	*7.059*	*10.827*	*2.391*	*5.560*	*8.970*	*20.309*	*3.258*	*4.083*
56.1	3.79	1	−1	2.323	4.044	8.113	9.633	6.618	8.773	2.150	3.652	9.177	20.684	3.550	4.369
				2.347	*4.001*	*8.083*	*9.596*	*6.489*	*9.191*	*2.132*	*3.885*	*9.221*	*20.753*	*3.582*	*4.400*
56.1	26.71	1	1	3.745	4.110	8.161	9.747	6.556	9.808	2.280	5.847	9.079	20.764	3.402	4.225
				3.700	*4.140*	*8.178*	*9.759*	*6.597*	*9.822*	*2.291*	*5.691*	*9.068*	*20.756*	*3.394*	*4.216*
60/0	15.25	1.2872	0	3.523	4.095	8.126	9.674	6.457	9.265	2.260	5.354	9.116	20.736	3.490	4.308
				3.557	*4.076*	*8.156*	*9.680*	*6.464*	*9.488*	*2.244*	*5.427*	*9.096*	*20.697*	*3.476*	*4.295*

As the center point of the experimental design was run twice, the total number of design points is 10.

(model 2) [6,7]:

$$\ln k'(x, y) = \ln\left(\frac{t - t_0}{t_0}\right) = \beta'_0 + \beta'_1 x + \beta'_2 y + \beta'_3 xy + \beta'_4 x^2 \beta'_5 y^2 \quad (7)$$

In the case of ion exclusion chromatography of weak acids, the capacity factor exhibits a Michaelis–Menten-like relationship with proton concentration, and thus the sulfuric acid concentration C [24]:

$$k'(C) = \gamma_0\left(\frac{C}{C + \gamma_1}\right) \quad (8)$$

where γ_0 is a constant absorbing the volumes of the mobile and resin phases, and γ_1 is related to the acid dissociation constant. The logarithm of the capacity factor is also expected to vary linearly with the reciprocal of absolute temperature over a small range [23]:

$$\ln k'(T) = \gamma_2 + \frac{\gamma_3}{T} \text{ or } k'(T) = \exp\left(\gamma_2 + \frac{\gamma_3}{T}\right) \quad (9)$$

Combining the functional forms of the T- and C-dependence of the capacity factor, a semi empirical model for the net retention time t' can be formulated as follows (model 3):

$$t'(x, y) = t - t_0 = \gamma_0\left(\frac{C}{C + \gamma_1}\right)\exp\left(\gamma_2 + \frac{\gamma_3}{T}\right) \quad (10)$$

The fitted variable t' is amenable for optimization/evaluation of $R_{i,j}$ values, as the dead time (t_0) cancels out upon subtraction. However, retention time estimates are preferably reported in absolute terms (t), which amounts to a correction with t_0. Models 1 and 2 were fitted according to the general linear model, using JMP 5.0.1. Fitting of model 3 was done using the solver routine in Microsoft Excel.

3. Results and discussion

3.1. Fitting of experimental data to retention model

Goodness of fit of models 1–3 to the retention data is assessed by the adjusted correlation coefficients as reported in Table 2. The adjusted correlation coefficient allows for comparison of models with different degrees of freedom [21]:

$$R^2_{\text{adj}} = 1 - (1 - R^2)\left(\frac{n - 1}{n - d}\right) \quad (11)$$

where R is the correlation coefficient, n the number of observations ($n = 10$ in this case), and d is the number of fitted parameters ($d = 6$ for models 1 and 2, $d = 4$ for model 3).

Although quadratic modeling of $\ln k'$ (model 2) has been widely used [6,7], it is not the best option here because the fit is the poorest for all compounds. Model 1 fits the data better than model 2, but the fit for acidic compounds is poor. Model 3 greatly improves the fit for acidic compounds. The fit for sugar and alcohol compounds is slightly better with model 1 than model 3. Based on these results, model 1 is used for sugars and alcohols, and model 3 is used for the acidic compounds. Comparison of predicted and actual values of net retention time t' at the design points (Table 1) shows good agreement, which would yet improve upon correction with t_0 (approximately 8.6 min) for comparison of actual retention time t.

Table 2
Goodness of fit assessment of three retention models

	R^2_{adj} (model 1)	R^2_{adj} (model 2)	R^2_{adj} (model 3)
Phosphate	0.9157	0.7269	0.9774
Malic acid	0.3917	0.2049	0.9871
Lactic acid	0.0910	−0.3612	0.9850
Formic acid	0.3641	0.0402	0.9961
Succinic acid	0.6762	0.5987	0.9724
Fumaric acid	0.4772	0.3443	0.9311
Citric acid	0.3751	0.2210	0.9900
Pyruvic acid	0.8260	0.5915	0.9813
Glucose	0.9552	0.9466	0.8892
Xylose	0.9571	0.9446	0.8945
Ethanol	0.9901	0.9671	0.9291
Glycerol	0.9202	0.9079	0.9589

Model 3 greatly improves the fit of acidic compounds.

3.2. Introduction and characterization of a novel quality criteria function

In this work an alternative to the classical global resolution function is proposed. The function is based on the pair-wise resolution $R_{i,j}$ as described in Eq. (1), only that the reciprocal is used:

$$R'_{i,j}\frac{(w_i/2) + (w_j/2)}{t_j - t_i} \quad (12)$$

Accordingly, the global resolution function here is defined as the sum of $R'_{i,j}$:

$$S = \sum_{i=1}^{n-1} R'_{i,i+1} \quad (13)$$

where $i = 1$ to n is peak index in order of appearance in the chromatogram. To our knowledge, such global resolution function has never appeared in the literature on HPLC optimization and therefore merits thorough evaluation. There are other quality criteria functions that are not based on $R_{i,j}$, e.g., peak separation [25] and overlapped fraction [26], but they do not allow for straightforward comparison with S. In the interest of presenting clear-cut comparisons, this discussion will be limited to $R_{i,j}$-based functions.

Many quality criteria functions based on the sum of $R_{i,j}$ (not $R'_{i,j}$ as used here) have been reported [10,11]. In the

simplest case, these functions take the following form:

$$R_s = \sum_{i=1}^{n-1} R_{i,i+1} = \sum_{i=1}^{n-1} \frac{t_{i+1} - t_i}{(w_{i+1}/2) + (w_i/2)} \quad (14)$$

It is obvious that in the special case where all w_i's are equal, R_s collapses to $(t_n - t_1)/w$, i.e., the inner peaks totally lose their significance. It is therefore not clear whether such functions correctly reflect favorable separation conditions for HPLC optimization.

With R_s-based functions, there is a need to limit the contribution of very well-separated pairs. This is not necessary for S, as well-separated pairs actually contribute the least. Each term in Eq. (13) can be thought of as punitive. If a pair is well-separated, its contribution is insignificant compared to the penalty due to an overlapping pair. There is no need for an arbitrary 'cut-off' value; peak pair contributions nicely balance themselves due to hyperbolic decay with respect to peak separation/distance.

Comparison of S with R_p shows that the characteristic property is retained, i.e., S also reaches an extremum (a minimum in this case) when all of the peaks are most evenly spaced. Unlike R_p, however, information on individual pairwise contributions is conserved in S. This is because each additive term in Eq. (13) is a positive number, whereas if the logarithm is applied to R_p in Eq. (2),

$$\ln R_p = \sum_{i=1}^{n-1} \ln R_{i,i+1} \quad (15)$$

the additive terms could be positive or negative, hence the "masking" effect. As mentioned before, this problem could be avoided by only considering the worst-separated pair (R_{min} [12] or α_{min} [6]) at the risk of losing critical information. Such sacrifice is not necessary with S, as all peak pairs do contribute without the masking effect.

Some R_p-based functions are normalized so that the values are bounded between 0 and 1 [27,28]:

$$R'_p = \prod_{i=1}^{n-1} \left[\frac{R_{i,i+1}}{1/(n-1)\sum_{i=1}^{n-1} R_{i,i+1}} \right]$$

$$= \frac{\prod_{i=1}^{n-1} R_{i,i+1}}{\left(1/(n-1)\sum_{i=1}^{n-1} R_{i,i+1}\right)^{n-1}} = \frac{\prod_{i=1}^{n-1} R_{i,i+1}}{\overline{R}^{n-1}} \quad (16)$$

where $\overline{R}$ is the mean resolution. As $\overline{R}$ is constant within a chromatogram, the form of R'_p in the last expression tells us that it also suffers the same masking effect as R_p. Moreover, from the first expression it is evident that when all $R_{i,i+1}$ terms are equal, R'_p reduces to unity regardless of the $R_{i,i+1}$ values. That means according to R'_p, a chromatogram with all $R_{i,i+1}$ values equal to 0.5 (not resolved) and one with all $R_{i,i+1}$ values equal to 2 (baseline resolved) are equally good, whereas they are of course not. These observations suggest that R'_p does not accurately reflect favorable conditions for chromatographic separation.

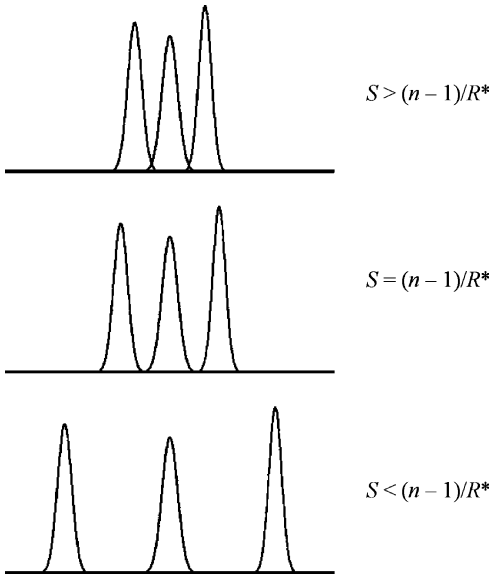

Fig. 2. Progression of peaks from overlapping to well-separated, with a limiting overlap as a hypothetical state. At this state the peaks are barely separated, and individual peak pairs contribute to $S = (n-1)/R^*$. As separation is better when $S \leq (n-1)/R^*$, $S > (n-1)/R^*$ is rejected because it is worse than limiting overlap.

These comparisons show how S is superior to general classes of quality criteria functions (R_s, R_p, and R_{min}), albeit having the same classical resolution function $R_{i,j}$ as its basis. Correct assessment of favorable separation conditions, preservation of individual peak pair contributions, and elimination of arbitrary cut-off values clearly make S an attractive choice for a quality criteria function.

At first glance, the switch from Eq. (1) to (12) would seem to introduce a problem when $t_i = t_j$, as now $R'_{i,j}$ would go to infinity. This is true. In fact, if there are n compounds in the sample, there could be $n(n-1)/2$ surface loci where S becomes infinity, effectively creating impenetrable barriers in the x–y domain. However, this should not hinder the visualization of S, as explained below.

Fig. 2 shows a progression of three chromatographic peaks from overlapping to well-separated. The middle state is a hypothetical situation ("limiting overlap") in which all of the peaks are barely separated, one appearing right next to another. In this case $S = (n-1)/R^*$ exactly, assuming peak symmetry and an (arbitrarily chosen) baseline resolution criterion of two adjacent peaks, R^*. If the system evolves from limiting overlap to a better separation, then $S \leq (n-1)/R^*$. By the same token, if $S > (n-1)/R^*$, then the separation must be worse than the limiting overlap (i.e., unacceptable). Therefore, $S > (n-1)/R^*$ can be used as a rejection criterion when visualizing S. In other words $(n-1)/R^*$ is effectively set as the upper limit of S, thereby ignoring singularities when $t_i = t_j$ in Eq. (12). However, $S < (n-1)/R^*$ does not necessarily mean that the separation is better than limiting overlap. Also, $S \leq (n-1)/R^*$ might not be feasible at all if there are too

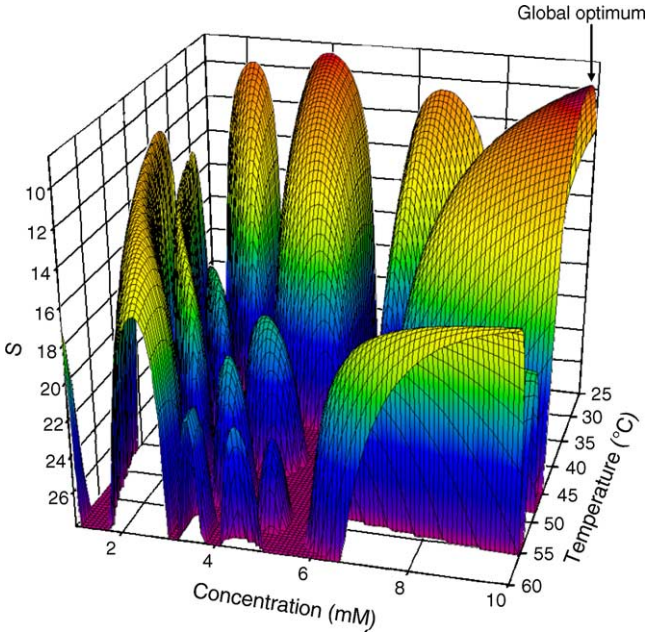

Fig. 3. The quality criteria function S for a hypothetical sample containing glucose, xylose, pyruvic acid, malic acid, formic acid, fumaric acid, and glycerol ($n = 7$). The direction of the S axis is reversed for ease visualization. A rejection criterion $S > 28$ is shown. Topology of S exhibits disconnected regions with many local optima.

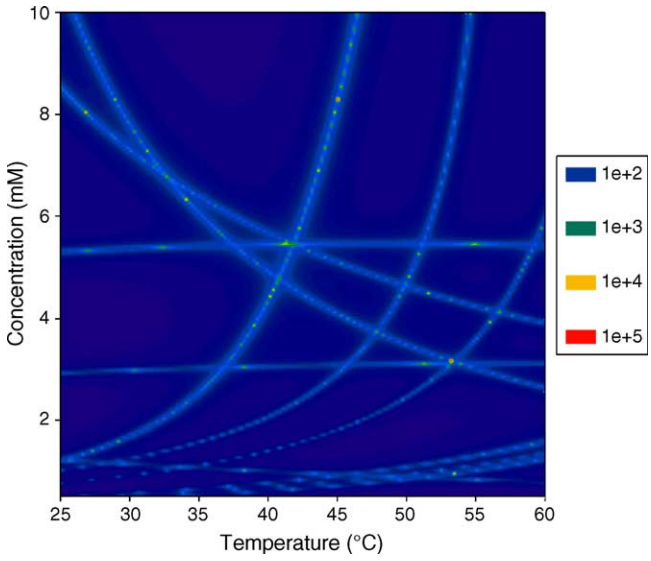

Fig. 4. The pathological domain of S. Contour plot shown corresponds to all 12 compounds. Each line indicates a pairwise coelution locus. When two lines cross, it means that four (non-unique) compounds are coeluting at that condition. The existence of disconnected regions in the domain results in many local minima, but the search algorithm should be able to identify only one true global optimum.

many compounds present in the sample (i.e., overcrowding of peaks in the chromatogram), in which case a less stringent rejection criterion may be chosen. It should be noted that this rejection criterion does not in any way affect the location of the global optimum, and therefore should not be confused with the resolution cut-off value in R_s that does affect the global optimum.

Revisiting the limiting overlap (Fig. 2), it is clear that the inequality $S \leq (n-1)/R^*$ is a result of inherently simple peak series geometry. A direct consequence of this nice feature is that given the number of compounds n, the absolute significance of S values can be readily assessed. That is, if $S > (n-1)/R^*$, one knows that there is peak overlap.

Fig. 3 shows a surface plot of S for a hypothetical sample containing glucose, xylose, pyruvic acid, malic acid, formic acid, fumaric acid, and glycerol ($n = 7$). For ease of visualization, the direction of the S axis is inverted. A global optimum ($S = 8.68$, $T = 32.0\,^{\circ}\mathrm{C}$, $C = 10.0$ mM) and 13 local optima are shown. Also evident in Figure is a rejection criterion $S > 28$.

As visualization of S by surface plots requires truncation at the rejection criterion, such plots can appear deceptively simple. The asymptotic nature of S is better represented in contour plots. Fig. 4 shows a contour plot of S for a sample having all 12 compounds (see Section 2.2). This "birds-eye view" shows a highly pathological domain with many local minima, defined by boundaries of the $t_i = t_j$ loci. Each line in Figure represents a singularity at which a "wall" of infinite height resides. These coelution loci effectively partition the domain into disconnected regions, with each region having at least one local optimum. This trait is apparent in Fig. 3. Although the disconnected regions (asymptotically) coalesce as $S \to \infty$, it is not possible to construct a continuous path traveling from one region to another.

3.3. Development and characterization of a novel optimum search algorithm

The challenge for any optimum search method is to identify a global optimum. Success highly depends on the nature of the function evaluated, and for non-analytical functions, absolute confidence in identifying the true global optimum is generally not possible. To optimize a pathological function like S with disjointed domains (and thus many optima), a robust, fast, and high-precision algorithm is required. Here we have developed an iterative stochastic search (ISS) method for the search of global optimum. To our knowledge, the method has never appeared in the literature on HPLC optimization, and global optimization in general. The proposed algorithm is outlined as follows, for a two-dimensional case (Fig. 5):

(1) Generate m random points in the (x–y) domain. m should be a small number, just big enough to generate meaningful statistics.
(2) Sort the m points from best to worst (lowest to highest S) to form a list. This is initialization for 'storage points'.
(3) Generate N random points in the domain (N should be several orders of magnitude greater than m, and follow a uniform distribution [29]). Each time, compare the new point to the worst point in the list (with highest S). If the new point is better, update the worst point in the list, and sort the list again (equivalent to insertion of the new

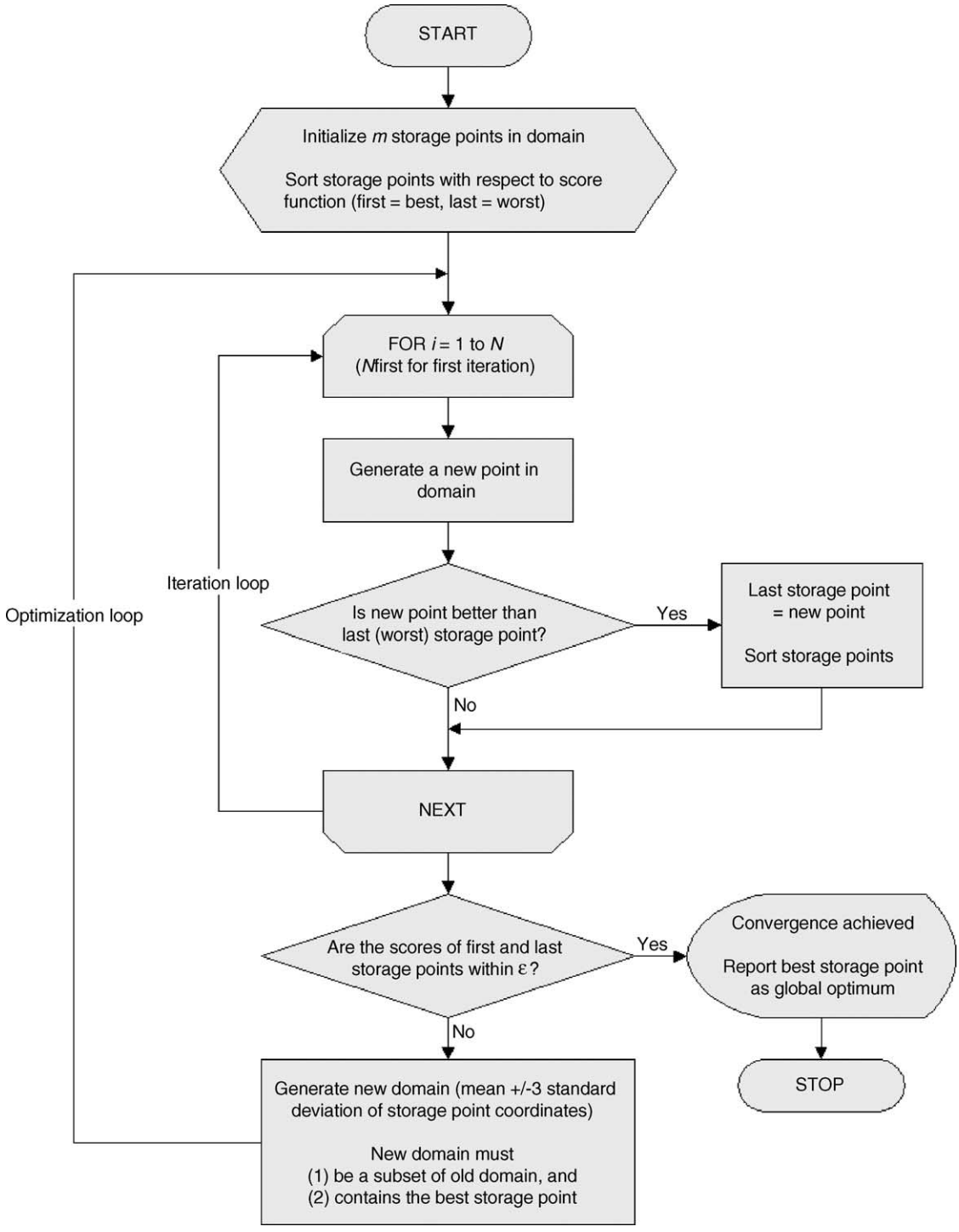

Fig. 5. The iterative stochastic search (ISS) algorithm is based on pure random search, in which cloud of uniformly distributed random points are evaluated within the domain. However, vast improvement in the convergence is achieved by successively shrinking the domain. In each iteration, the new, smaller domain is generated based on the best storage points of the previous iteration. Each iteration in the ISS algorithm essentially identifies *m* best points out of *N* points. This can be achieved simply by sorting the *N* points directly, but such implementation would be computationally demanding and require large storage memory. The 'on-demand' sorting algorithm operating on a small list (*m* elements) minimizes CPU and memory load while achieving the same result.

point). If this is the first iteration, instead of N use N_{first} (one or two orders of magnitude greater than N).
(4) If the best and worst points in the list are equally good (S values within a predetermined tolerance ε), stop the search. The best point in the list is identified as the global optimum. If not, continue.
(5) Calculate the mean and standard deviation for the x and y coordinates of the points in the list.
(6) Generate a new (smaller) domain as the mean ± 3SD for the x and y coordinates. The new domain must satisfy two requirements: it must be a subset of the old domain, and it must contain the best point in the current list. Otherwise, adjust the ranges accordingly.
(7) Go back to step 3.

In optimization of a continuous function $f(x)$, a necessary condition is that $\mathrm{d}f/\mathrm{d}x = 0$ at the optimum x^*, which translates to the convergence rule: given a small number $\varepsilon > 0$, there exists a δ such that $|f(x) - f(x^*)| < \varepsilon$ whenever $|x - x^*| < \delta$. In ISS, the use of m storage points allows for identification of a small convergence neighborhood around the global optimum such that precision is defined by ε, and confidence intervals by the smallest and largest storage point coordinates, which represent δ. Note that ε is chosen arbitrarily, but δ is a result of optimization. Of course ε cannot be smaller than the computer's floating-point precision (10^{-8}), and should not be too large as to making two distinct optima indistinguishable. An ideal choice for ε would be the standard error estimate for the optimized function at the optimum, as a precision exceeding the expected error would not be meaningful. However, this requires a priori knowledge of the optimum (which is yet to be found), and an exhaustive traceback of error propagation from the original chromatograms, model fitting, and function evaluations, which seems like unnecessary labor.

Each iteration in the ISS algorithm essentially identifies m best points out of N points. This can be achieved simply by sorting the N points directly, but such implementation would be computationally demanding and require large storage memory. The 'on-demand' sorting algorithm operating on a small list (m elements) minimizes CPU and memory load while achieving the same result.

The first iteration is the most critical. In this step, more points (N_{first}) are generated to ensure that the whole domain is sampled more thoroughly. At the end of the first iteration, the m best points should already cluster around the neighborhood of the global optimum. Statistical measures of the m best points (center of mass, standard deviation) are then used to define a new, smaller domain for the second iteration (the choice of a $\pm 3\sigma$ span is conservative in a sense that if the m sample points come from a normally distributed population, the entire population is represented within $\mu \pm 3\sigma$). As such, subsequent iterations are done over smaller (and shrinking) domains surrounding the global optimum, until finally all of the m best points are within a small tolerance ε, at which point the global optimum is identified.

The shrinking domain is analogous to serial dilution of a concentrated liquid sample. By serial dilution, the same degree of dilution can be achieved using less amount of diluent. In this case, the same degree of precision can be achieved by generating fewer points total. Therefore, N should not be too large as to cause oversampling (because only a fraction of the generated points are accepted), but also not too small as to cause unrepresentative sampling.

ISS is similar to grid search (GS) in that it samples the domain homogeneously, but through generation of N random points instead of grid construction. To compare GS and ISS, consider the point density ρ (defined as N/domain volume) for the last iteration where convergence is obtained. For GS to have the same precision as ISS, it must have the same point density, but applied to the whole original domain volume V_0. Therefore, the ratio of points generated (and evaluated) in GS to ISS ($r_{\text{GS,ISS}}$) is calculated as:

$$r_{\text{GS,ISS}} = \frac{\rho V_0}{(n_{\text{iter}} - 1)N + N_{\text{first}}} = \frac{N(V_0/V_{\text{f}})}{(n_{\text{iter}} - 1)N + N_{\text{first}}} = \frac{V_0/V_{\text{f}}}{(n_{\text{iter}} - 1) + (N_{\text{first}}/N)} \quad (17)$$

where n_{iter} is the number of iterations and V_{f} is the final domain volume at the last iteration.

Although it is not possible to obtain a general value for n_{iter}, our experience with the current system (see Section 3.4) shows that it is normally below 100, even for the most difficult case (all compounds included in optimization). As N_{first} is also about two orders of magnitude higher than N, the denominator of Eq. (17) should be in the order of 100 or less. However, the numerator V_0/V_{f} is very large because the upper and lower bounds of each dimension (x or y) becomes asymptotically close at the end of iteration, and depending on the convergence criterion ε, can be approaching machine precision (10^{-8}). This would make the ratio $r_{\text{GS,ISS}}$ (and thus computation time) prohibitively large, proving that GS can never achieve the same degree of precision as ISS. Note that grid size itself should not be confused with precision (ε) in the sense of convergence ($\mathrm{d}f/\mathrm{d}x = 0$). Although grid size serves as a measure of grid quality, grid construction is akin to choosing an arbitrary δ, instead of obtaining it by choosing ε in the convergence rule.

The choice of grid size is arbitrary, but probably best guided by the precision of instruments (not to be confused by the convergence precision, ε) used in, or for the preparation of the experiments. For example, grid size for a temperature axis could be set to the smallest increment in the temperature controller, e.g., 0.1 °C. An example of this is given in Section 3.6.

From a convergence (precision and confidence) standpoint, the simplex search (SS) is analogous to ISS in that the $d + 1$ vertices also serve as storage points. SS is a sequential algorithm (path-dependent) that climbs downhill in the quality criteria function field. Although SS is a fast algorithm, by design it converges to the nearest local optimum, instead of global optimum. This problem is overcome in ISS by thor-

ough sampling (N_{first} points) of the entire domain in the first iteration.

The simulated annealing (SA) method was used in a recent example of HPLC optimization [7]. SA is a widely used global optimization technique that mimics the metallurgical process of annealing (slow cooling). The algorithm consists of a random walk within the simulation domain, with each trial move accepted with probability of 1 if it is downhill (criteria function improves), but follows the Maxwell–Boltzmann distribution otherwise [29]. A nonzero probability of accepting uphill moves allows the optimization path to climb out of local optima. However, as the Boltzmann factor vanishes with gradual lowering of system 'temperature', uphill moves become less likely and eventually the path only goes downhill in the vicinity of the global optimum.

Although ISS bears a resemblance to SA in that both rely on a stochastic factor in the progression toward the global optimum, the two algorithms are fundamentally different. The optimization path in SA is a Markov chain, in which the next position in the path is dependent on the current position [30]. Thus, when the path encounters a local optimum, it cannot escape immediately but rather oscillates until the ridge is reached, resulting in futile cycles. At early stages of the simulation, such wasteful oscillations may even occur around the (then indistinguishable) global optimum. In ISS, the next position in the optimization sequence is independent of the current position (random search, not random walk). Progression toward the global optimum is therefore not subject to spatial restrictions governing a path/chain, but allowed to explore the entire domain freely and uniformly. Within a Markov chain of length N, a fraction could be wasted in SA due to futile cycles, but all N points will contribute to the uniform sampling of the simulation domain in ISS, resulting in identification of m best points for the next iteration.

For a successful implementation of SA, many parameters such as length of Markov chain, initial step size and temperature, coefficients for temperature and step size decrement (cooling schedule), and threshold criteria (stopping rule) [30,31] need to be fine-tuned to best suit the behavior of the quality criteria function and volume of the simulation domain. In contrast, ISS implementation only involves N_{first}, N, and m. Furthermore, as m is known to be small so as to facilitate fast sorting, fine tuning is only needed for N_{first} and N. From a practical standpoint, ISS is clearly an easier algorithm.

Characterization of ISS reveals interesting analogies (i.e., storage points, uniform sampling, stochastic processes) to algorithms commonly used in HPLC optimization (SS, GS, and SA). In each case, however, ISS features clear advantages (e.g., ability to identify global optimum, higher precision, more efficient use of CPU cycles, easier implementation), thus making it an attractive choice as an optimum search method.

As a final note, it is possible to use stopping criteria (step 4 in ISS algorithm) other than the mathematical definition of ε–δ convergence. For example, the search can be stopped when all of the coordinates/independent variables are within predetermined instrument precisions (e.g., 0.1 °C for temperature), or when within an iteration, all of the N generated new points are no better than the existing m points in the list.

3.4. Implementation of the proposed optimization method

A computer program (OPTIMIZE) was written in Visual Basic 6 (Microsoft, Redmond, WA) for automated optimum identification, based on the alternative global resolution function S and the search algorithm ISS described above. The program uses model coefficients for retention times as described previously (Section 3.1). Although the model is specific to the column used (Bio-Rad HPX-87H), retention models for other columns can easily be substituted.

In optimization, values for m and N are set to 20 and 2000, respectively. N_{first} is calculated as follows:

$$N_{first} = \max\left(N,\ \frac{n(n-1)}{n_{max}(n_{max}-1)} \times 100,000\right) \tag{18}$$

where n is the number of compounds and n_{max} is the maximum number of compounds (=12). The $n(n-1)$ factor effectively scales N_{first} according to the number of possible pair coelution loci. For example, N_{first} = 100,000 if n = 12. If n = 6, N_{first} is only 22,727.

3.5. Application of iterative stochastic search method to higher dimensional problems

From the algorithm description, it is evident that ISS can be easily generalized to more than two dimensions. The method can be tested using a periodic, hyperdimensional function with many optima,

$$F_1(\boldsymbol{x}) = \prod_{i=1}^{d} \frac{\cos x_i}{e^{0.01x_i^2}} \tag{19}$$

and also the non-periodic version,

$$F_2(\boldsymbol{x}) = \prod_{i=1}^{d} \frac{1}{e^{0.01x_i^2}} \tag{20}$$

where $\boldsymbol{x}$ is the vector of independent variables and d is the number of dimensions/independent variables. Fig. 6 shows F_1 for the two-dimensional case (d = 2), whereas F_2 would be a simple mound-shaped surface. Both F_1 and F_2 assume a global optimum value of 1 at $\boldsymbol{x}$ = [0].

The choice of N_{first} and N depends on the number of dimensions, and also the hyperdimensional volume of the domain evaluated. As each variable x_i is evaluated in $[-z, z]$, the volume V is calculated as $(2z)^d$. A maximum volume V_0 is chosen at z = 20. N_{first} is set to $(V/V_0)10^{d-1}$, but restricted in [10,000,1,000,000]. N is set to min(10,000, N_{first}/50).

The search algorithm was coded in Visual Basic 6 and executed on a 2.0 GHz Pentium 4 PC. Correct identification of the global optimum is achieved in all trial runs ($\varepsilon = 10^{-5}$,

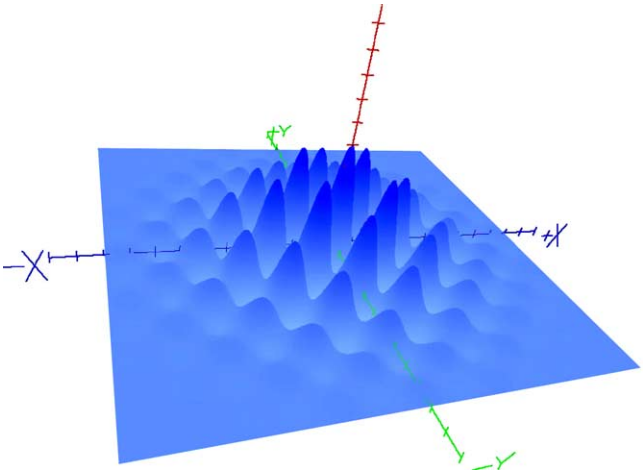

Fig. 6. Periodic function F_1 in 2 dimensions (x and y), drawn in $[-z, z] = [-20, 20]$. The z-direction here is scaled up 10 times to clearly show the optima. The function reaches a global optimum at (0, 0).The function F_2 (not shown) would look like a mound centered at the origin, tangent to the optima of F_1.

$z = 10$). Reasonable simulation time (under 1 min) is achieved up to $d = 7$ for F_1. Optimization of F_2 is much faster because of the simpler form of the function. At $d = 7$, F_2 is optimized within 0.2 s.

Although hypothetical functions F_1 and F_2 are different in form compared to real quality criteria functions (e.g., S), they are representative of "difficult" and "easy" hyperdimensional functions. F_1 is certainly as difficult as any real quality criteria function, so robust performance of ISS up to seven dimensions here looks promising, suggesting potential application in HPLC optimization in larger dimensional spaces (e.g., temperature, flow rate, pH, ionic strength, tertiary mobile phase composition). To our knowledge, there has been no simultaneous HPLC optimization reported in the literature that operates on more than four dimensions. The availability of more robust (faster and more accurate) search algorithms such as ISS may provide an incentive for higher dimensional optimization in HPLC separation.

3.6. Identification of optimal and pathological conditions using proposed optimization method

Execution of the overall optimization strategy (experimental design, modeling, scoring, and optimum identification) is demonstrated on a sample containing representative substrates and products found in microbial fermentation processes. The sample contained 0.1 g/L each of potassium phosphate (KH_2PO_4), glucose, xylose, malic acid, succinic acid, lactic acid, formic acid, and ethanol (eight compounds). Based on the retention model and peak width estimates from a preliminary run, the optimal conditions were identified using OPTIMIZE: $T = 26.1\,^{\circ}C$ and $C = 6.57$ mM, with analysis time ~30 min based on ethanol as the last eluting compound. The optimized run is shown in Fig. 7a. The retention times are in excellent agreement with the predicted values according to the retention model (all within 1%). The actual S value of 7.224 compares well with the predicted value of 7.610 (within 5%).

The ISS algorithm used solved the optimization problem in 0.25 s through 50,444 evaluations of S, at $\varepsilon = 10^{-7}$ (2.0 GHz Pentium 4 PC). For comparison, consider a GS with grid size approximating instrument precisions. The smallest increment in the temperature controller is $0.1\,^{\circ}C$, so the number of grids in the x-direction is $(60\,^{\circ}C - 25\,^{\circ}C)/(0.1\,^{\circ}C) = 350$. Assuming 18 M H_2SO_4 for prepa-

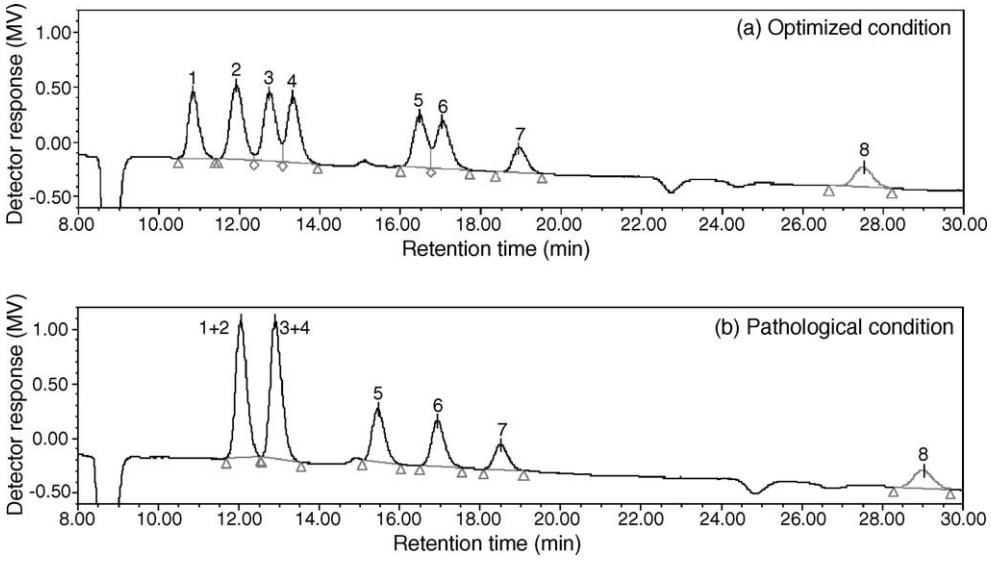

Fig. 7. HPLC separation of a sample containing 0.1 g/L each of (1) potassium phosphate (KH_2PO_4), (2) glucose, (3) xylose, (4) malic acid, (5) succinic acid, (6) lactic acid, (7) formic acid, and (8) ethanol, in the order of elution times. (a). Optimized/best condition at $T = 26.1\,^{\circ}C$ and $C = 6.57$ mM. (b) Pathological/worst condition at $T = 50.6\,^{\circ}C$ and $C = 17.84$ mM. Here phosphate coelutes with glucose and xylose coelutes with malic acid.

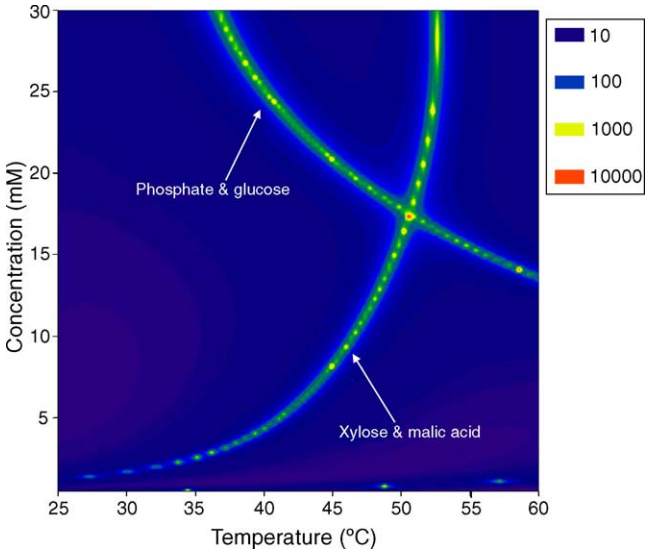

Fig. 8. Contour plot of quality criteria function S for a sample containing phosphate, glucose, xylose, malic acid, succinic acid, lactic acid, formic acid, and ethanol ($n = 8$). Two coelution loci shown correspond to phosphate and glucose, and xylose and malic acid. These two loci intersect at $T = 50.6\,^{\circ}C$ and $C = 17.84$ mM.

ration of 1 L of mobile phase using a micropipetter with 1 μL increments, the number of grids in the y-direction = (30–0.5 mM)(1000 mL/18,000 mM)(1000 μL/mL) = 1639. With total number of grid points = (350 + 1)(1639 + 1) = 575,640 function evaluations, the problem was optimized in 2.63 s. The speedup factor of ISS over GS is >10 times in this case.

The retention model allows us not only to predict the optimal condition, but in a sense also to avoid pathological conditions. For this set of compounds, there are two coelution loci, i.e., phosphate-glucose and xylose–malic acid. Fig. 8 shows that these two loci/lines cross at $T = 50.6\,^{\circ}C$ and $C = 17.84$ mM, at which phosphate would coelute with glucose and xylose would coelute with malic acid. The sample was run at this condition, and the coelutions occur as predicted (Fig. 7b). Comparison of Fig. 7a and b demonstrates that the choice of temperature and solvent concentration can produce strikingly different results. The optimized run still has partial overlaps (solvable through deconvolution using chromatogram analysis packages), but the pathological run has two complete overlaps, which means that not only two, but four (50%) compounds are unquantifiable. All the same, this shows how the retention model used was able to accurately predict both the best and worst operating conditions for a particular sample.

As a side note, the fact that even the optimum or best possible chromatographic separation in this case still has partial overlaps attests to the need for optimization. Of course, on the other hand optimization may not be needed at all in cases where the peaks are always baseline resolved.

4. Conclusions

The alternative global resolution function S for HPLC optimization proposed in this work shows superior performance when compared to general classes of quality criteria functions (R_s, R_p, and R_{min}), including correct assessment of favorable separation conditions, preservation of individual peak pair contributions, elimination of arbitrary cut-off values, and a unique capability to interpret absolute significance of function values through a simple inequality. The novel global optimization algorithm (iterative stochastic search, ISS) also developed in this work shows clear advantages over existing algorithms for HPLC optimization (grid search, simplex search, simulated annealing) in its ability to correctly identify the global optimum (instead of local optimum), with higher precision, with more efficient use of computation cycles, and with easier implementation. Based on a case study using a hyperdimensional function with many optima, robust performance of ISS also suggests its possible application in simultaneous, higher-dimensional HPLC optimization. Successful application of S and ISS to HPLC optimization was demonstrated in the separation of 8 representative substrates and products found in microbial fermentation. Excellent agreement was found between actual and predicted values for the optimized (best) and pathological (worst) conditions. The overall optimization strategy successfully implemented in this work can be generalized to any HPLC optimization problem.

Acknowledgements

This project was supported by grants from the US National Science Foundation (BES-0331388), the US Department of Agriculture (2004-35505-14193), and the US Department of Energy (DEFG3603GO13159). The authors wish to thank Mr. Ganesh Sriram of the ISU Department of Chemical Engineering for suggestions in constructing periodic functions.

References

[1] Q.-S. Wang, R.-Y. Gao, B.-W. Yan, D.-P. Fan, Chromatographia 38 (1994) 187.
[2] J. Qiu, J. Chromatogr. A 859 (1999) 153.
[3] X.-G. Chen, X. Li, L. Kong, J.-Y. Ni, R.-H. Zhao, H.-F. Zou, Chemom. Intell. Lab. Syst. 27 (2003) 157.
[4] S.D. Patterson, J. Chromatogr. 592 (1992) 43.
[5] K. Outinen, H. Haario, P. Vuorela, M. Nyman, E. Ukkonen, H. Vuorela, Eur. J. Pharm. Sci. 6 (1998) 197.
[6] V. Harang, A. Karlsson, M. Josefson, Chromatographia 54 (2001) 703.
[7] Y.C. Guillaume, E. Peyrin, Talanta 51 (2000) 579.
[8] B. Bourguignon, F. Marcenac, H.R. Keller, P.F. de Aguiar, D.L. Massart, J. Chromatogr. 628 (1993) 171.
[9] P.J. Schoenmakers, A.C.J.H. Drouen, H.A.H. Billiet, L. Degalan, Chromatographia 15 (1982) 688.

[10] J.L. Glajch, J.J. Kirkland, K.M. Squire, J.M. Minor, J. Chromatogr. 199 (1980) 57.
[11] J.C. Berridge, J. Chromatogr. 244 (1982) 1.
[12] Y. Guillaume, E.J. Cavalli, E. Peyrin, C. Guinchard, J. Liq. Chromatogr. Rel. Technol. 20 (1997) 1741.
[13] H.J.G. Debets, J. Liq. Chromatogr. 8 (1985) 2725.
[14] E.J. Klein, S.L. Rivera, J. Liq. Chromatogr. Relat. Technol. 23 (2000) 2097.
[15] S.N. Deming, M.L.H. Turoff, Anal. Chem. 50 (1978) 546.
[16] S. Srijaranai, R. Burakham, R.L. Deming, T. Khammeng, Talanta 56 (2002) 655.
[17] N. Kuppithayanant, M. Rayanakorn, S. Wongpornchai, T. Prapamontol, R.L. Deming, Talanta 61 (2003) 879.
[18] M.C. Gennaro, E. Marengo, V. Gianotti, S. Angioi, J. Chromatogr. A 945 (2002) 287.
[19] E. Marengo, V. Gianotti, S. Angioi, M.C. Gennaro, J. Chromatogr. A 1029 (2004) 57.
[20] A.V. Pirogov, O.N. Obrezkov, O.A. Shpigun, J. Anal. Chem. 52 (1997) 918.
[21] A.I. Khuri, J.A. Cornell, Response Surfaces: Designs and Analyses, second ed., Marcel Dekker, New York, 1996.
[22] A.L. Medved', A.A. Ivanov, O.A. Shipgun, J. Anal. Chem. 52 (1997) 39.
[23] J. Weiss, Ion Chromatogr., VCH, Weinheim, 1995.
[24] E. Papp, P. Keresztes, J. Chromatogr. 506 (1990) 157.
[25] M.W. Watson, P.W. Carr, Anal. Chem. 51 (1979) 1835.
[26] S. Carda-Broch, J.R. Torres-Lapasió, M.C. García-Alvarez-Coque, Anal. Chim. Acta 396 (1999) 61.
[27] Vivó-Truyols, J.R. Torres-Lapasió, M.C. García-Alvarez-Coque, J. Chromatogr. A 991 (2003) 47.
[28] S. Sekulic, P.R. Haddad, J. Chromatogr. 485 (1989) 501.
[29] W.H. Press, B.P. Flannery, S.A. Teukolsky, W.T. Vetterling, Numerical Recipes in Fortran, second ed., Cambridge University Press, New York, 1992.
[30] P.J.M. van Laarhoven, E.H.L. Aarts, Simulated Annealing: Theory and Applications, D. Reidel Publ., Dordrecht, 1987.
[31] B. Hajek, Math. Oper. Res. 13 (1988) 311.